Synthetic Metals 189 (2014) 177–182

Contents lists available at ScienceDirect

Synthetic Metals

journal homepage: www.elsevier.com/locate/synmet

Investigating thermoelectric properties of doped polyaniline nanowires

Jiansheng Wu [a], Yimeng Sun [b], Wei Xu [b,**], Qichun Zhang [a,*]

[a] School of Materials Science and Engineering, Nanyang Technological University, 50 Nanyang Avenue, Singapore 639672, Singapore
[b] Beijing National Laboratory for Molecular Sciences, Laboratory of Organic Solids, Institute of Chemistry, Chinese Academy of Sciences, Beijing 100190, PR China

ARTICLE INFO

Article history:
Received 19 November 2013
Received in revised form 7 January 2014
Accepted 10 January 2014
Available online 4 February 2014

Keywords:
Electrical conductivity
Nanostructures
Polymers
Thermal conductivity
Thermoelectric effects

ABSTRACT

Polyaniline (PANI) nanostructures doped with different acids have been prepared through a soft template method. The structures, morphologies and thermoelectric (TE) properties of the as-prepared PANI nanostructures have been carefully investigated. Our results showed that doping level, types of doping acids, and morphologies of as-prepared nanostructures did have strong effect on TE properties. For example, we found that higher doping level in HCl-doped PANI nanowires did not give better thermoelectric performance although it is true in some curtain doping range. AcOH-doped samples became worse than HCl-doped ones due to the poor doping ability of AcOH. As to p-toluenesulfonic acid (p-TSA) doped nanowires, ZT value is 2.75×10^{-5} at 300 K, which is 4 times higher than that of HCl-doped one because doped bulky anions make PANI chains more order. As to the morphology effect, two p-TSA doped samples (nanowires and nanorods) at the same doping level were prepared and the nanowires showed the better Seebeck coefficient and lower thermal conductivity. Comparing with nanorods, Seebeck coefficient of nanowires increased 164% while thermal conductivity reduced by 25% for nanowires. The ZT value for nanowires is 5 times higher than that of nanorods.

1. Introduction

Thermoelectric (TE) devices based on one-dimensional (1D) organic crystalline nanostructures have attracted a lot of scientific interests because theoretical calculation shows that *ZT* (an important factor to evaluate TE materials) for both p- and n-type materials at room temperature may reach ~20 if quasi 1D organic crystals could linearly stack into one chain and then furthermore pack into a 3D crystal [1,2]. Although organic TE materials (most are TE polymers) cannot compete with inorganic PE materials in medium and high temperature, they do have a lot of applications in *on-demand* cooling and low-end waste heat management [3]. In addition, organic TE materials (most are TE polymers) do have some charming properties such as low density, low thermal conductivity, low cost, and easy to synthesis or process [4,5].

There are three factors (electrical conductivity (σ), Seebeck coefficient (S), and thermal conductivity (κ)) to determine the performance of TE polymers [6]. According to the equation $ZT = (S^2\sigma/\kappa)^*T$, one might conclude that higher conductivity, larger Seebeck, and lower thermal conductivity would give a larger *ZT*. Unfortunately, three variable factors are somewhat interdependent in bulk materials. Such conflicting makes optimization of *ZT* more challenging and more difficult. Interestingly, recent researches have demonstrated that nano-engineering in materials might break this limitation. Especially, nanostructured conjugated polymers show a better performance as TE materials [7].

The conductivities of conjugated polymers are strongly dependent on structural factors, oxidation state (non-doping, p-doping, or n-doping), and morphology (crystalline or non-crystalline). Generally, plain conjugated polymers have semiconducting or even insulting properties. In order to make conjugated polymers useful in TE devices, a doping process is required. There are a lot of ways to dope conjugated polymers including electrochemical doping, chemical doping, photodoping, charge injection doping, and doping by acid–base treatment. After doping, the properties of conducting polymers could be switched from the insulating state (less than 10^{-10} S cm^{-1}) to the metallic regime (large than 10^2 S cm^{-1}), which is good enough for TE applications [8].

Polyaniline (PANI) as one of the important conducting polymers has caused a lot of scientists' interests due to high stability, facile synthesis and tunable electronic properties [9]. Since the conductivities of PANI are strongly affected by its doping levels and the doping agents, systematic study on the relation between thermoelectric behaviors and the doping process is very important. In this report, we are more interested in the TE performance of doped PANI

* Corresponding author. Tel.: +65 67904705; fax: +65 67909081.
** Corresponding author.
E-mail addresses: wxu@iccas.ac.cn (W. Xu), qczhang@ntu.edu.sg (Q. Zhang).

0379-6779/$ – see front matter © 2014 Elsevier B.V. All rights reserved.
http://dx.doi.org/10.1016/j.synthmet.2014.01.007

nanowires. We have systematically studied how the doping level and doping agents affect the TE properties of PANI nanowires.

2. Experimental

2.1. Chemicals

Aniline monomer and APS were purchased from Alfa Aeser Company. CTAB and p-toluenesulfonic acid (p-TSA) were purchased from Sigma–Aldrich Company. Hydrochloric acid (HCl), acetic acid (AcOH), acetone and ethanol were purchased from Merck Millipore Company. Aniline monomer was distilled under low pressure before use and other chemicals were directly used as received. Deionized water used in all experiments was produced with the Millipore S. A. 67120 apparatus.

2.2. PANI nanowires preparation

The HCl doped PANI nanowires were prepared by using soft template method. 0.5 mL (5 mmol) aniline monomer and 0.1 g CTAB were dissolved in 50 mL HCl solution. 1.14 g (5 mmol) APS was dissolved in 10 mL HCl solution. Then, the two solutions were mixed rapidly and stirred for 12 h in an ice bath (0–5 °C). The mixture was filtered in a Buchner funnel. After that the dark-green precipitate was washed with ethanol, acetone and deionized water for several times respectively. Finally, the HCl doped PANI nanowires were dried in vacuum at 60 °C for 24 h. The AcOH and p-TSA doped HCl nanowires were prepared in a similar processing. Because of some white floccules appear in the solution before the polymerization in an ice bath, the p-TSA doped PANI wide nanorods were obtained. Therefore, the p-TSA doped PANI nanowires were prepared at room temperature.

2.3. Characterization

FT-IR spectra were recorded on a PerkinElmer Spectrum BX FTIR spectrometer. FESEM was performed on a JEOL/JSM-6340F with an acceleration voltage of 5 kV.

2.4. Thermoelectric properties measurement

The Seebeck coefficient, electrical conductivity, thermal conductivity were measured by SB-100 Seebeck Measurement System (MMR Tech.), KEITHLEY 2002 Multimeter (Keithley Instrument Inc.), TCi Thermal Conductivity Analyzer (C-THERM Tech.), respectively. The samples were compressed into a disk shape pellet with diameters of 17 mm, and thickness of 1–2 mm for thermoconductivity measurement, then they were cut into rectangle shape (2 mm × 5 mm) for electrical conductivity and Seebeck coefficient measurement.

3. Results and discussion

3.1. Characterization of structures and morphologies

PANI nanowires doped with different acids were prepared by using soft template method. Herein, the aniline monomer was polymerized using ammonium persulfate (APS) as oxidant, hexadecyl trimethyl ammonium bromide (CTAB) as soft template and different acids (AcOH, HCl, and p-TSA) as dopants. The FT-IR spectra have been employed to characterize the structure of the main chain of different acid-doped PANI nanowires. As shown in Fig. 1, all doped PANI samples showed strong bands at 1563 cm^{-1}, 1486 cm^{-1}, 1294 cm^{-1}, and 1116 cm^{-1}, which can be assigned to the C=C stretching of quinoid rings, C=C stretching of benzenoid rings, C—N stretching of secondary aromatic amine, and aromatic C—H in-plane bending, respectively [10]. The AcOH-doped PANI samples have an absorption peak at 1040 cm^{-1}, which comes from the C—O stretching of the AcO^- group, while the p-TSA doped PANI samples showed bands at 1032 cm^{-1} and 1008 cm^{-1}, which are assigned to the S=O stretching of the p-TSA group. The results confirmed that both AcOH and p-TSA have successfully doped in PANI chains. The band at 1116 cm^{-1} is considered as the electronic-like band, a measurement of the degree of delocalization of electrons on PANI, which is the characteristic peak of PANI conductivity [11]. In the spectrum of AcOH doped PANI, the weak band at 1116 cm^{-1} might imply a poor doping and a poor electrical conductivity. For 0.1 M HCl doped PANI nanowires, the vibrations bands at 1563 and 1486 cm^{-1} in FT-IR spectrum indicate fewer quinoid units in PANI chain [12]. It may reduce the sample's electrical conductivity. The PANI nanowires doped with 0.5 and 1.0 M HCl show the complete conjugated structure. Compare their absorption intensity at 1116 cm^{-1} in FT-IR spectrum, the doping level of PANI nanowires doped with 1.0 M HCl is higher than that of the other one.

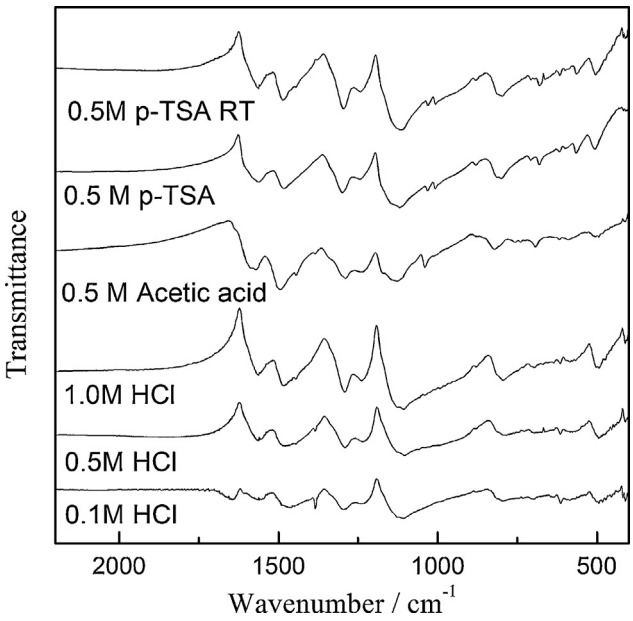

Fig. 1. FT-IR spectra of different acid doped PANI samples.

The morphologies of different acid doped PANI nanowires have been investigated through SEM and the results are shown in Fig. 2. Fig. 2a–c shows the images of PANI nanowires with 0.1, 0.5, and 1.0 M HCl doping concentration, respectively. The diameters of doped PANI wires are about 120 nm for 0.1 M HCl, 100 nm for 0.5 M HCl and 80 nm for 1 M HCl respectively. It is worthy to note that there are some particles appeared in 0.1 M HCl-doped nanowires, indicating that low concentration of HCl might limit the polymerization process. This conclusion is further supported by the FT-IR spectra of HCl (0.1 M) doped PANI nanowires (Fig. 1), where the weaker bands at 1563 and 1486 cm^{-1} could be investigated, indicating the smaller conjugation level of PANI main chains [13]. The morphology of AcOH (0.5 M) doped PANI nanowires (Fig. 2d) is similar to those of HCl doped ones. The diameter for AcOH (0.5 M) doped PANI nanowires is about 70 nm. Interestingly, the morphologies of p-TSA doped PANI nanowires depend on the synthetic temperatures. As shown in Fig. 2e and f, p-TSA doped PANI nanostructures prepared in an ice bath (0–5 °C) have nanorod shape with the diameter of about 150 nm while room temperature gave p-TSA doped PANI nanowires with the diameter of 70 nm. Such results might be attributed to the poor solubility of p-TSA at low temperature.

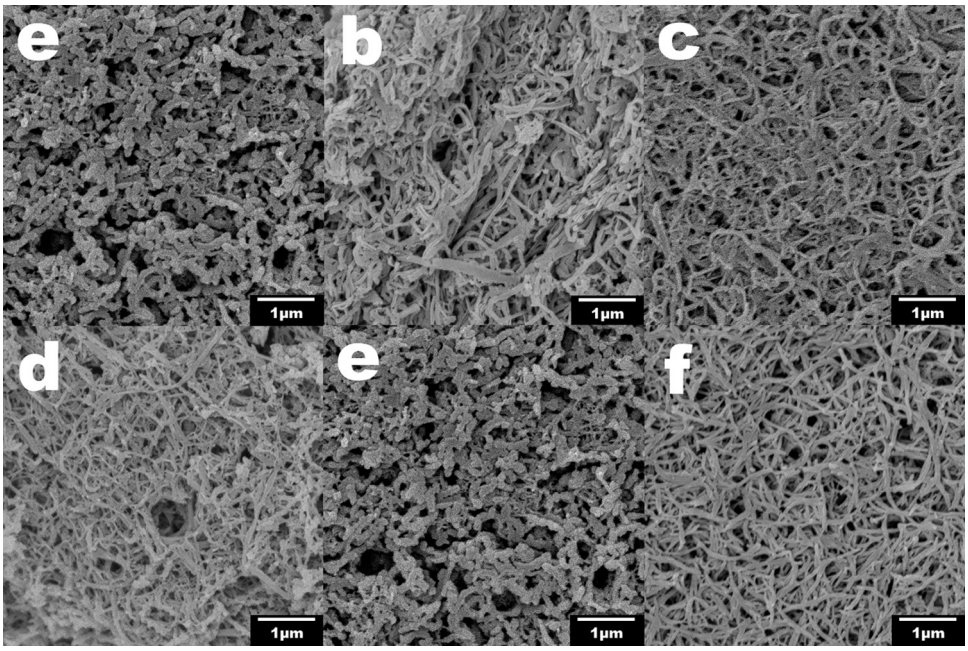

Fig. 2. SEM images of (a–c) HCl (0.1, 0.5, 1.0 M) doped PANI nanowires; (d) AcOH (0.5 M) doped PANI nanowires; (e) p-TSA (0.5 M) doped PANI irregular nanorods; (f) p-TSA (0.5 M) doped PANI nanowires.

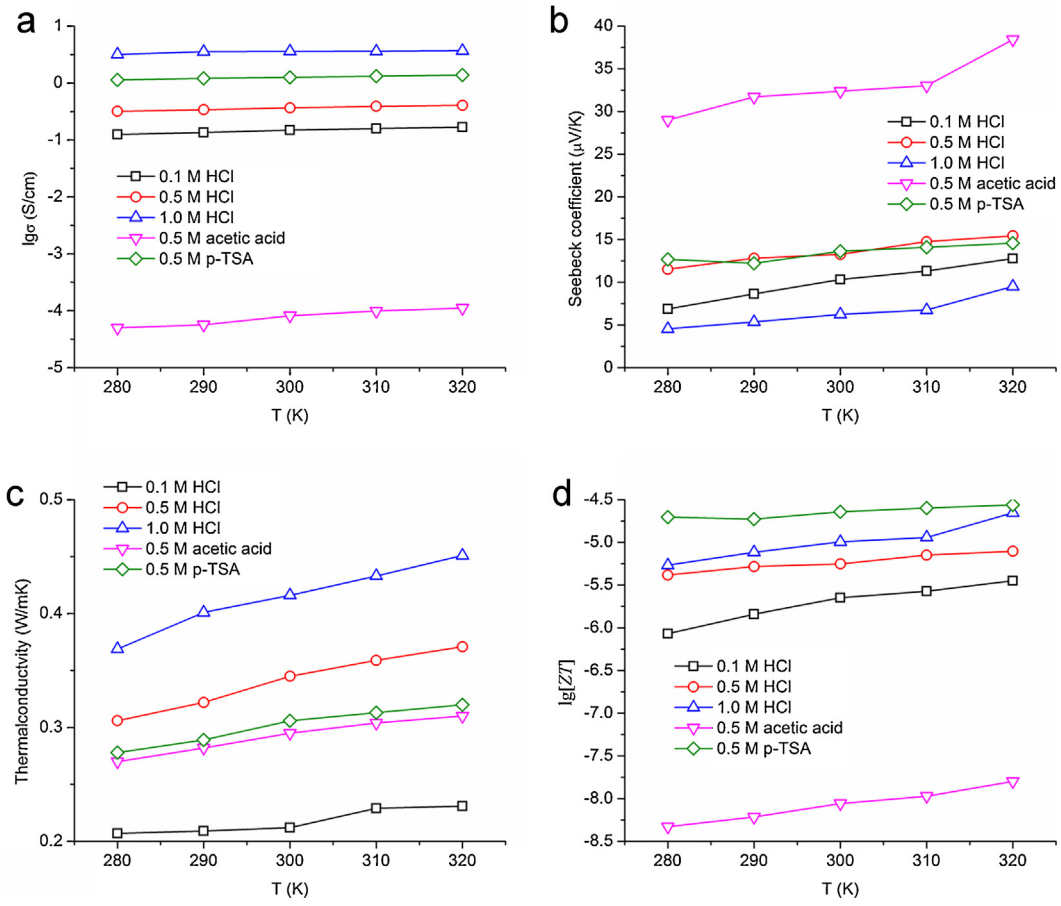

Fig. 3. The temperature (T) dependence of (a) electrical conductivity (σ); (b) Seebeck coefficient; (c) thermal conductivity; (d) figure-of-merit *ZT* of different acid doped PANI nanowires.

3.2. Thermoelectric properties of PANI nanowires affected by different acids and the doping level

The temperature (T) dependence of electrical conductivities (σ) of different acid doped PANI nanowires is shown in Fig. 3a. Generally, undoped PANI is an insulator ($\sigma < 10^{-9}$ S cm^{-1}). With the increasing doping levels, it can be gradually switched from an insulator to a semiconductor or even metallic. All of the doped PANI nanowires show an organic semiconductor characteristic, which is that the electrical conductivity increased with the rise of temperature [14]. The electrical conductivities of HCl-doped PANI nanowires increased with the rise of HCl concentration and range from 10^{-1} to 10 S cm^{-1}. Although p-TSA (0.5 M) doped PANI nanowires shows a similar electrical conductivity about 1 S cm^{-1}. The electrical conductivity of AcOH doped PANI nanowires is very poor (about 10^{-4} S cm^{-1}).

It is well known that the electrical conductivity of a semiconductor can be given by the following Eq. (1) [15]:

$$\sigma = ne\mu \quad (1)$$

where n is carrier concentration (doping level), e is electric charge, and μ is carrier mobility. Since Polarons are the main carriers for doped PANI, all electric charges of doped PANI nanowires are almost same. Thus, the disparity of electrical conductivity should be dependant on the concentration of different carriers and their mobilities. When HCl concentration increases, more H^+ proton can bond with =N— in main chain of PANI and more carriers can be formed, leading to the enhancement of the electrical conductivity. The p-TSA is a strong organic acid with a large p-toluenesulfonic group. Although p-TSA provides fewer H^+ protons (low carrier concentration) comparing to HCl, the p-TSA doped PANI nanowires have higher carrier mobility because the large volume of p-toluenesulfonic group can improve the regularity of PANI molecule through acting as counter anions around the main chain of PANI [16,17]. Therefore, the electrical conductivity of p-TSA doped PANI nanowires is higher than that of PANI doped with HCl at the same concentration. It is not surprising to find that the electrical conductivity of AcOH-doped PANI nanowires is only about 10^{-4} S cm^{-1} because of AcOH is a weak acid and it cannot provide enough H^+ protons to increase carrier concentration.

Fig. 3b shows the temperature dependence of Seebeck coefficients of different acid doped PANI nanowires. The positive values of all samples indicated that all acid-doped PANI nanowires are p-type organic semiconductors. Since increasing carrier concentration generally results in the increasing of electrical conductivity and the decreasing of Seebeck coefficient, it is not surprising that the Seebeck coefficients of AcOH doped PANI nanowires is about 2–3 times higher than those of other PANI nanowires. In fact, previous researches about TE behaviors of PANI have already indicated that the conductivity increased and the Seebeck coefficient decreased when the doping levels increased [11]. Therefore, the high Seebeck coefficient of AcOH-doped PANI nanowires should be caused by its low doping level. Although HCl (1.0 M)-doped PANI nanowires showed highest electrical conductivity and the lowest Seebeck coefficient, it is noteworthy that PANI nanowires with various concentration HCl-doping did not follow this trend. For example, electrical conductivity and Seebeck coefficient of 0.5 M HCl-doped PANI nanowires are higher than those of 0.1 M HCl-doped PANI nanowires. The reason for such results lies in the fact that the PANI nanowires prepared at 0.1 M HCl concentration show a poor quality of nanowires (Fig. 2a, some particles around the nanowires). Previously, it was also observed that the Seebeck coefficient and electrical conductivity increased simultaneously in the PANI nanotubes, which can be accounted by the enhanced carrier mobility resulted from the improved molecular ordering of polymer chains [18]. The conclusion could be further supported by p-TSA doped PANI nanowires, which have a higher Seebeck coefficient and relatively higher electrical conductivity. Since all Seebeck coefficients of PANI nanowires increased with the increasing of temperature, all PANI samples are not the typical semiconductor behaviors but similar to the diffusive metallic thermopower.

Thermal conductivities of all doped PANI nanowires were also studied and the temperature dependence of thermal conductivities were shown in Fig. 3c. Clearly, all the thermal conductivities of PANI nanowires follow the well-known theory that the thermal conductivities of amorphous solids increases with temperature rising [18]. The thermal conductivity of different acid doped PANI nanowires range from 0.2 to 0.4 W m^{-1} K^{-1}, which are slightly higher that those of most conductive polymers (about 0.1 W m^{-1} K^{-1}). In general, the thermal conductivity of PANI is insensitive to the preparation or doping conditions, but it is easy to be affected by environment [19].

The TE figure of merit, ZT, is also calculated and compared. As shown in Fig. 3d, the ZT values of all doped PANI nanowires increases with the temperature rising. Because of the relatively higher electrical conductivity and Seebeck coefficient, the p-TSA doped PANI nanowires show the highest ZT value (2.75×10^{-5} at 300 K). For any doped PANI nanowires, there is a balance between electrical conductivity and Seebeck coefficient.

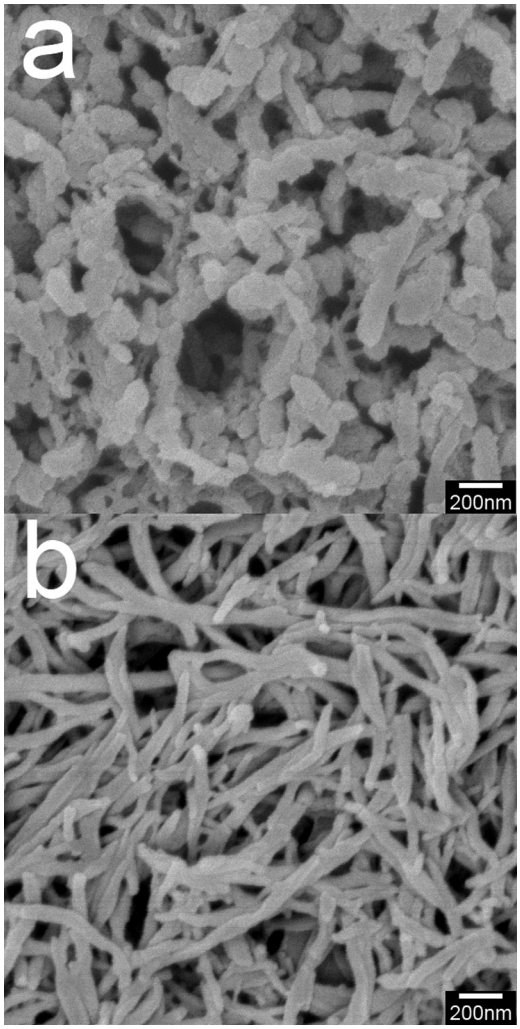

Fig. 4. SEM images of (a) PANI nanorods prepared in an ice bath; (b) PANI nanowires prepared at room temperature.

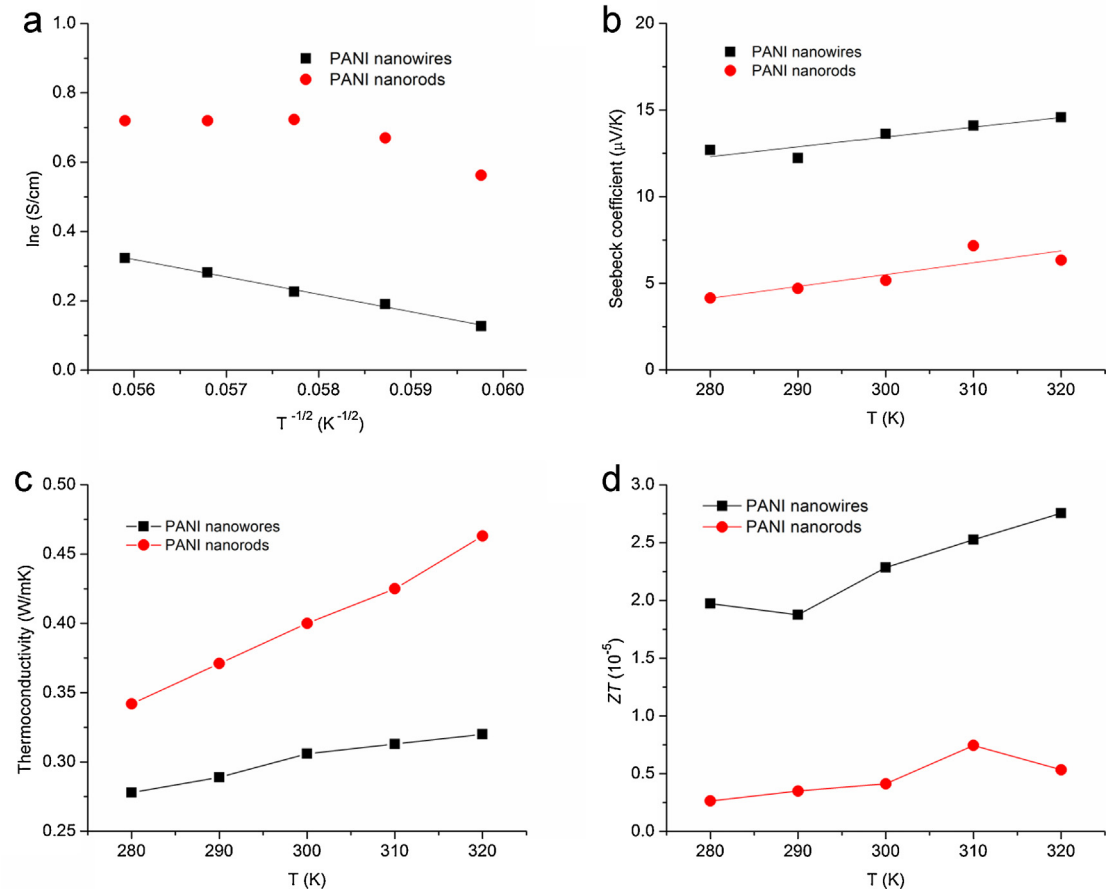

Fig. 5. The temperature (T) dependence of (a) electrical conductivities (σ); (b) Seebeck coefficient; (c) thermal conductivity; (d) figure-of-merit ZT of p-TSA doped PANI nanowires and nanorods.

3.3. Thermoelectric properties of PANI affected by morphologies

Using different temperature to prepare p-TSA doped PANI gave two different morphologies: nanowires for room temperature and nanorods for ice bath (Fig. 4). The length of most rods varied from 200 to 1000 nm while the average diameter was around 150 nm. The morphology of nanowires is more regular than the nanorods. Its diameter is about 70 nm and length is about 1–2 μm.

Although the FT-IR spectra in Fig. 1 have already confirmed that nanowires and nanorods have the similar doping level, the TE parameters of two samples were different. The electrical conductivities of PANI nanowires and nanorods at room temperature are 1.25 and 2.06 S cm^{-1}, respectively. Fig. 5a shows the temperature dependence of electrical conductivities for two samples. It is interesting to point that the PANI nanowires show a good linear relationship between the ln(σ) and the $T^{-1/2}$, indicating the charge transport of PANI nanowires follows the quasi-one-dimensional variable range hopping (1D-VRH) model (Eq. (2)):

$$\sigma(T) = \sigma_0 \exp\left[-\left(\frac{T_0}{T}\right)^{1/2}\right] \quad (2)$$

where σ_0 is a constant, T_0 is the characteristic Mott temperature that generally depends on the carrier hopping barriers [20]. But, the electrical conductivity of PANI nanorods did not follow this model. This is because the irregular structure of PANI main chain may impede the hoping.

Fig. 5b shows the temperature dependence of Seebeck coefficients of two samples. The Seebeck coefficients of both samples increase slightly with temperature rising. It is noteworthy that the Seebeck coefficient of the nanowires is about 2–3 times higher than that of nanorods. This result might imply that smaller diameters and more regular nanostructures have some contribution to the larger Seebeck coefficient of PANI nanowires. Such a result could also be attributed to the enhanced charge carrier mobility resulted from the improved molecular ordering of polymer chains.

The temperature-dependent thermal conductivities of two samples were also studied and were shown in Fig. 5c. The thermal conductivities of two samples increased with the temperature rising. However, the thermal conductivity of nanowires is lower than that of nanorods. Generally, the thermal conductivity contributes from two parts: the carriers' conductivity (κ_{car}) and phonons' (κ_{ph}), as the following description (Eq. (3)):

$$\kappa = \kappa_{car} + \kappa_{ph} \quad (3)$$

In most of conductive polymers, κ_{ph} is the main contribution to thermal conductivity [21]. As shown in SEM images (Fig. 4), the PANI nanowires are strongly bent and entwined. This morphology can increase the boundary phonon scattering at the interface in the heat transfer process. In addition, the smaller diameter could block the transport of phonons by producing huge superficial area among the nanowires. Therefore, the small diameter of nanowires would give a lower thermal conductivity at different temperatures comparing to nanorods or larger wires.

The ZT value of two samples were also calculated and shown in Fig. 5d. Because of the higher Seebeck coefficient and lower thermal

conductivity, the *ZT* value of PANI nanowires is about 5 times higher than that of nanorods.

4. Conclusion

The different acid doped PANI samples have been successfully prepared through soft template method and their morphologies and TE performances have been studied. The electrical conductivity, Seebeck coefficients and thermal conductivity results show that p-toluenesulfonic acid (p-TSA) is the best dopant among three different acids because bulky p-toluenesulfonic anions make PANI chains more order. AcOH-doped samples show poorest performance due to the weak doping ability of AcOH. In addition, at the same doping level, p-TSA-doped nanowires showed the better Seebeck coefficient and lower thermal conductivity than p-TSA-doped nanorods. Our research could be instructive to study other organic TE systems.

Acknowledgements

Q.Z. acknowledges financial support from AcRF Tier 1 (RG 16/12) and Tier 2 (ARC 20/12 and ARC 2/13) from MOE, the CREATE program (Nanomaterials for Energy and Water Management) from NRF, and the New Initiative Fund from NTU, Singapore. X.W thanks the support from National Natural Science Foundation of China (21021091 and 21333011).

References

[1] M.S. Dresselhaus, G. Chen, M.Y. Tang, R.G. Yang, H. Lee, D.Z. Wang, Z.F. Ren, J.P. Fleurial, P. Gogna, New directions for low-dimensional thermoelectric materials, Adv. Mater. 19 (2007) 1043–1053.
[2] M.G. Kanatzidis, Nanostructured thermoelectrics the new paradigm? Chem. Mater. 22 (2009) 648–659.
[3] N. Dubey, M. Leclerc, Conducting polymers: efficient thermoelectric materials, J. Polym. Sci. B: Polym. Phys. 49 (2011) 467–475.
[4] J. Yang, H.-L. Yip, A.K.Y. Jen, Rational design of advanced thermoelectric materials, Adv. Energy Mater. 3 (2013) 549–565.
[5] A.B. Kaiser, V. Skakalova, Electronic conduction in polymers, carbon nanotubes and graphene, Chem. Soc. Rev. 40 (2011) 3786–3801.
[6] M. He, F. Qiu, Z. Lin, Towards high-performance polymer-based thermoelectric materials, Energy Environ. Sci. 6 (2013) 1352–1361.
[7] Y. Du, S.Z. Shen, K. Cai, P.S. Casey, Research progress on polymer–inorganic thermoelectric nanocomposite materials, Prog. Polym. Sci. 37 (2012) 820–841.
[8] O. Bubnova, X. Crispin, Towards polymer-based organic thermoelectric generators, Energy Environ. Sci. 5 (2012) 9345–9362.
[9] M. Jaymand, Recent progress in chemical modification of polyaniline, Prog. Polym. Sci. 38 (2013) 1287–1306.
[10] S.-A. Chen, H.-T. Lee, Structure and properties of poly(acrylic acid)-doped polyaniline, Macromolecules 28 (1995) 2858–2866.
[11] J. Li, X. Tang, H. Li, Y. Yan, Q. Zhang, Synthesis and thermoelectric properties of hydrochloric acid-doped polyaniline, Synth. Met. 160 (2010) 1153–1158.
[12] K.L. Tan, B.T.G. Tan, E.T. Kang, K.G. Neoh, X-ray photoelectron spectroscopy studies of the chemical structure of polyaniline, Phys. Rev. B 39 (1989) 8070–8073.
[13] F. Yan, G. Xue, Synthesis and characterization of electrically conducting polyaniline in water–oil microemulsion, J. Mater. Chem. 9 (1999) 3035–3039.
[14] D. Emin, T. Holstein, Adiabatic theory of an electron in a deformable continuum, Phys. Rev. Lett. 36 (1976) 323–326.
[15] D. Emin, Pair breaking in semiclassical singlet small-bipolaron hopping, Phys. Rev. B 53 (1996) 1260–1268.
[16] M.M. Ayad, E.A. Zaki, Doping of polyaniline films with organic sulfonic acids in aqueous media and the effect of water on these doped films, Eur. Polym. J. 44 (2008) 3741–3747.
[17] V.I. Krinichnyi, H.K. Roth, M. Schrödner, B. Wessling, EPR study of polyaniline highly doped by p-toluenesulfonic acid, Polymer 47 (2006) 7460–7468.
[18] Y. Sun, Z. Wei, W. Xu, D. Zhu, A three-in-one improvement in thermoelectric properties of polyaniline brought by nanostructures, Synth. Met. 160 (2010) 2371–2376.
[19] H. Yan, N. Ohno, N. Toshima, Low thermal conductivities of undoped and various protonic acid-doped polyaniline films, Chem. Lett. 29 (2000) 392–393.
[20] Z.H. Wang, E.M. Scherr, A.G. MacDiarmid, A.J. Epstein, Transport and EPR studies of polyaniline: a quasi-one-dimensional conductor with three-dimensional "metallic" states, Phys. Rev. B 45 (1992) 4190–4202.
[21] Z. Han, A. Fina, Thermal conductivity of carbon nanotubes and their polymer nanocomposites: a review, Prog. Polym. Sci. 36 (2011) 914–944.